

# Vibration of Cantilevered Rectangular Plates with Circular Ends- A Study in Mode Shapes

C.Y. Wang

*Departments of Mathematics and Mechanical Engineering Michigan State University, East Lansing, MI 48824, USA*

## Abstract

The vibrations of rectangular plates with circular ends, including the completely free stadium- shaped plate, the long cantilever plate and the wide cantilever plate are studied for the first time. Accurate archival frequencies and mode shapes are obtained by the Ritz method. In comparison to rectangular plates with the same area, the rounded rectangular plate has less boundary length and structurally stronger, while the frequencies change little. The vibration shapes show distinct flapping modes and twisting modes.

**Keywords:** *Plate; Vibration; Free; Cantilever; Frequency; Mode.*

## 1. Introduction

The study of the vibration of plates is essential in structural design. Exact solutions may exist if the boundary of the plate can be described by separable coordinates [1]. Otherwise numerical or semi- numerical means are necessary [2, 3].

The aim of the present paper is to study the free vibration of a rectangular plates with circular ends. Since the sharp corners of the rectangular plate are absent, this geometry is favorable in terms of both strength and material savings. The first case of our study is the completely free vibration of the stadium- shaped plate (Figure 1a). Practical applications include solar panels orbiting in space [4], large floating marine platforms [5], and lightly supported plates. The second case is the cantilever rectangular plates with free circular ends (Figure 1b, 1c). This case models cantilever ledges, propeller blades, aircraft wings etc.

The completely free vibration of circular, elliptic, rectangular, triangular plates have long been studied. See Leissa [2, 6] for the earlier works. Square plates with rounded corners were considered by Irie et al [7] using conformal mapping and the variational Ritz method. Recently Wang [8] studied homotopy shapes in between a rectangle and an ellipse. The last two sources used continuous functions to describe the boundary, which do not apply to the shapes studied in the present paper. On the other hand the stadium- shaped plate, having straight and circular boundaries, is easier to fabricate than elliptic or super-elliptic plates.

Vibrations of cantilever plates are of interest in the study of wing behavior. Rectangular, quadrilateral, triangular plates with one edge clamped and other edges free have been investigated [2]. Square or elliptic plates have also been considered [9, 10]. We shall study the more difficult cantilever rectangular plate with circular ends.

This geometry does not conform to separable coordinates. Also the boundary cannot be described by a single boundary function. Thus the methods of [7, 8] fail. Finite differences and finite elements can be used, but much effort is needed to accommodate the conditions of the curved

free edges. We shall use the powerful Ritz method which normally not applicable to piecewise continuous boundaries [11]. However, for free vibrations such boundary restrictions are relaxed and the Ritz method can be used.

We are interested in the natural frequencies and the vibration mode shapes of the rectangular plate with circular ends, which has never been studied before.

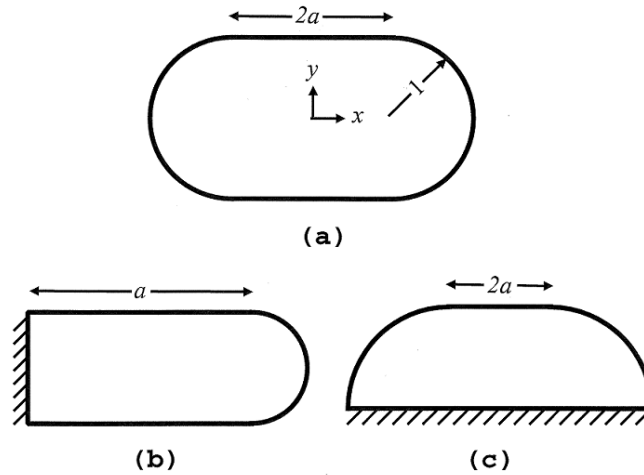


Figure1. (a) The completely free stadium- shaped plate (b) The long cantilever plate (c) The wide cantilever plate.

## 2. Method of solution

First consider the completely free stadium- shaped plate (Figure 1a). Normalize all lengths by the half width  $L$ , the thin plate vibration equation is [2]

$$\nabla^4 w - k^2 w = 0 \quad (1)$$

where  $w$  is the transverse displacement amplitude, and the normalized frequency is

$$k = \omega L^2 \sqrt{\frac{\rho h}{D}} \quad (2)$$

Here  $\omega$  is the frequency,  $\rho$  is the density,  $h$  is the thickness, and  $D$  is the flexural rigidity. The energy functional [12], with zero applied forces or moments, is simplified to

$$E = \frac{D}{2} \iint_{\Omega} [(w_{xx} + w_{yy})^2 + 2(1-\nu)(w_{xy}^2 - w_{xx}w_{yy})] dx dy - \frac{\rho h \omega^2}{2} \iint_{\Omega} w^2 dx dy \quad (3)$$

Here  $(x,y)$  are Cartesian coordinates, the integrals are over the area  $\Omega$  and the Poisson ratio  $\nu$  is set to 0.3 for our computations. The variation or minimization of  $E$  yields [13]

$$\delta E = D \iint_{\Omega} (\nabla^4 w - k^2 w) \delta w dx dy = 0 \quad (4)$$

Thus if  $w$  is arbitrary inside  $\Omega$ , Eq.(1) is recovered. For the Ritz method, let the displacement be expressed in a linear sum of Ritz functions  $\phi_i$ . The Ritz functions are complete and have no restrictions inside and on the free edges of the plate.

$$w = \sum_1^{\infty} c_i \phi_i(x, y) \quad (5)$$

Truncate Eq.(5) to  $N$  terms and minimize  $E$  with respect to the constant coefficients  $c_i$ . After

some work we find

$$\sum_{i=1}^N c_i (A_{ij} - k^2 B_{ij}) = 0 \quad (6)$$

where

$$A_{ij} = \iint_{\Omega} [\phi_{ixx} \phi_{jxx} + \phi_{iyy} \phi_{jyy} + 2(1-\nu)\phi_{ixy} \phi_{jxy} + \nu(\phi_{ixx} \phi_{jyy} + \phi_{jxx} \phi_{iyy})] dx dy \quad (7)$$

$$B_{ij} = \iint_{\Omega} \phi_i \phi_j dx dy$$

For non-trivial solutions, we set the determinant to zero:

$$|A_{ij} - k^2 B_{ij}| = 0 \quad (8)$$

Eq.(8) is the characteristic equation for the frequencies  $k$ . For each frequency, the coefficients  $c_i$  (up to a constant) can be obtained from Eq.(6) and the mode shapes from Eq.(5).

For the completely free plate in Fig.1a, let the normalized dimensions of the rectangle be  $2a$  by  $2$ , with semi-circular ends of radius  $1$ . Cartesian coordinates are placed at the centroid. Due to geometric symmetry, the vibration modes can only be the following four types: symmetric in both  $x$  and  $y$  directions (SS), symmetric in the  $x$  direction but anti-symmetric in the  $y$  direction (SA), anti-symmetric in the  $x$  direction but symmetric in the  $y$  direction (AS), or anti-symmetric in both directions (AA).

Let the Ritz functions be the polynomial set

$$\{\phi\} = q\{1, x^2, y^2, x^4, x^2 y^2, y^4, x^6, x^4 y^2, x^2 y^4, y^6, x^8, x^6 y^2, x^4 y^4, x^2 y^6, y^8 \dots\} \quad (9)$$

For the SS modes, we set  $q=1$ , for the SA modes  $q=y$ , for the AS modes  $q=x$ , and for the AA modes  $q=xy$ . The number of terms  $N$  taken are the highest homogeneous powers, i.e. 3, 6, 10, 15, 21, 28, 36, etc. Table 1 shows the convergence rate is fairly fast. That  $N=28$  would be sufficient for convergence.

Table 1. Typical convergence of frequency  $k$ . Empty cells denote the values have converged.

$N$	$a = 0.25$ 7 <sup>th</sup> mode AA	$a = 1$ 6 <sup>th</sup> mode SS	$a = 2$ 3 <sup>rd</sup> mode AS	$a = 5$ 5 <sup>th</sup> mode SA
10	16.157	6.0306	1.8252	1.1855
15	16.150	7.8747	1.8227	1.1853
21	16.148	7.8535	1.8227	1.1853
28	16.147	7.8505		
36	16.147	7.8504		

An accuracy test is the free vibration of a circular plate ( $a=0$ ) for which an exact solution exists. The frequencies of the completely free circular plate is [1]

$$\frac{\alpha^3 I_n'(\alpha) - (1-\nu)n^2 [\alpha I_n'(\alpha) - I_n(\alpha)]}{\alpha^2 I_n(\alpha) - (1-\nu)[\alpha I_n'(\alpha) - n^2 I_n(\alpha)]} = \frac{\alpha^3 J_n'(\alpha) + (1-\nu)n^2 [\alpha J_n'(\alpha) - J_n(\alpha)]}{\alpha^2 J_n(\alpha) + (1-\nu)[\alpha J_n'(\alpha) - n^2 J_n(\alpha)]} \quad (10)$$

Here  $\alpha = \sqrt{k}$ ,  $J_n, I_n$  are Bessel functions and modified Bessel functions of the first kind, and  $n$

is the number of diametrical nodal lines. Table 2 shows the convergence of our method to the exact values from Eq.(10). It is seen that our method is accurate to all five digits.

Table 2. Convergence of the frequencies for the completely free circular plate. Empty cells denote the values have converged. Exact values are from Eq.(10).

$N$	SS	AA	SS	AS	SA	AS	SA
10	5.3583	5.3583	9.0035	12.439	12.439	20.483	20.475
15	5.3583	5.3583	9.0031	12.439	12.439	20.475	20.475
21	5.3583	5.3583	9.0031			20.475	
28	5.3583	5.3584					
36	5.3584	5.3584					
Exact	5.3584	5.3584	9.0031	12.439	12.439	20.475	20.475

For the long cantilever plate of Figure 1b, the boundary is clamped on the minor axis at  $x = 0$ . Since there is no symmetry in the  $x$  direction, the Ritz functions are

$$\{\phi\} = qx^2 \{1, x, x^2, y^2, x^3, xy^2, x^4, x^2y^2, y^4, x^5, x^3y^2, xy^4, x^6, x^4y^2, x^2y^4, y^6 \dots\} \quad (11)$$

here  $q=1$  if the mode is symmetrical in  $y$  (S), and  $q=y$  if it is anti-symmetrical in  $y$  (A).

For the wide cantilever plate of Fig.1c, the boundary is clamped on the major axis at  $y=0$ . The Ritz functions are taken as

$$\{\phi\} = qy^2 \{1, y, x^2, y^2, y^3, x^2y, x^4, x^2y^2, y^4, y^5, y^3x^2, yx^4, x^6, x^4y^2, x^2y^4, y^6 \dots\} \quad (12)$$

where  $q=1$  if the mode is symmetrical in  $x$  (S), and  $q=x$  if it is anti-symmetrical in  $x$  (A). The convergence for both cantilever plates are similar to the completely free plate.

Another comparison is the semi-circular cantilever plate. The only published report is due to McGee et al [14] who also used a Ritz method to study the circular sector plate clamped at the straight edges. A special sector is the semi-circle which McGee et al [14] found the first six frequencies. Table 3 shows the differences between our results and theirs are less than 0.05%. On the other hand, Westmann [15] used a one-term Rayleigh quotient and obtained a less satisfactory 5.66 for the fundamental frequency.

Table 3. Comparison of the first six frequencies with the results of McGee et al [14] for the semi-circular cantilever plate.

present	4.5384	9.3561	17.229	27.016	27.581	40.264
Ref.[14]	4.5399	9.3519	17.222	27.037	27.565	40.235

### 3. Results

Table 4 shows the first eight frequencies of the completely free rectangular plate with semicircular ends. The frequencies for  $a = 0$  (circle) confirm Eq.(10). Some frequencies for the circular plate are the same when rotated a half period, for example AA and SS, also AS and SA.

Table 4 First eight frequencies of the completely free stadium- shaped plate. Aspect ratio is  $a+1$ . Subscripts denote mode shape.

$a$	0	0.25	0.5	1	2	3	4	5
$k$	5.358SS	3.890SS	2.789SS	1.564SS	0.671SS	0.368SS	0.231SS	0.159SS
	5.358AA	3.946AA	3.082AA	2.108AA	1.274AA	0.911AA	0.636AS	0.437AS
	9.003SS	7.265SS	6.605SS	4.094AS	1.823AS	1.009AS	0.709AA	0.580AA
	12.44AS	9.132AS	6.871AS	4.701SA	2.772SA	1.901SA	1.244SS	0.856SS
	12.44SA	9.239SA	7.103SA	6.015SS	3.493SS	1.962SS	1.460SA	1.185SA
	20.48AS	14.21AS	11.07AS	7.850SS	4.474AA	3.036AA	2.048AS	1.413AS
	20.48SA	16.15AA	12.42AA	8.074AA	5.539AS	3.208AS	2.290AA	1.838AA
	21.84SS	16.27SS	12.49SS	8.322AS	5.884SS	4.362SA	3.044SS	2.108SS

The corresponding mode shapes are also obtained, excluding spurious frequencies. Figure 2 shows the results. Note that the fundamental mode is always SS with two transverse nodal curves. The second mode is AA but switches to AS between  $a = 3$  and  $a = 4$ . Higher modes show more frequent switching of the mode orders. For very high aspect ratios we expect the modes alternate between SS and AS with transverse nodal curves. The frequencies decrease with increased aspect ratio or area.

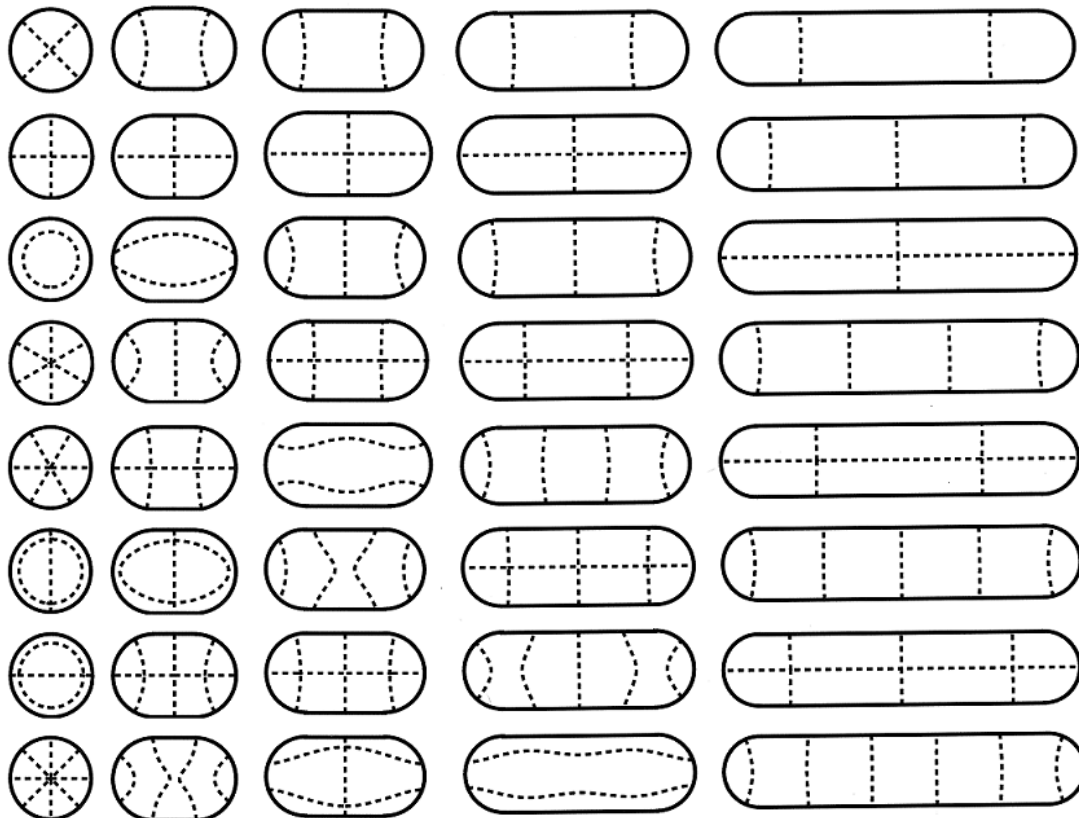


Figure 2. First eight vibration modes of the completely free stadium- shaped plate. Dashed lines denote nodal curves. From left:  $a = 0, 0.5, 1, 3, 5$ .

The frequencies of the long cantilever plate are given in Table 5. The subscript S denotes symmetry in the  $y$  direction, or the vibration is mainly up-and-down along the major axis. The subscript A denotes anti-symmetry in the  $y$  direction, or there exists a twisting motion about the  $x$  axis.

Table 5 First eight frequencies of the long cantilever plate. Aspect ratio is  $(a+1)/2$ . Subscripts denote mode shape.

$a$	0	0.5	1	2	3	4	5
$k$	4.5384S	1.939S	1.044S	0.438S	0.238S	0.149S	0.102S
	9.3561A	4.579A	2.845A	1.550A	1.051A	0.784A	0.631S
	17.229S	9.208S	5.675S	2.597S	1.448S	0.916S	0.635A
	27.016S	13.35S	9.211S	5.239A	3.449A	2.534S	1.752S
	27.581A	15.20A	9.790A	6.482S	3.944S	2.564A	2.007A
	40.264S	24.41A	14.62S	7.619S	6.381S	4.776A	3.370S
	41.950A	31.37A	18.62A	10.34A	6.606A	4.888S	3.648A
	55.191A	32.34S	19.87S	11.40S	7.547S	6.172S	4.383S

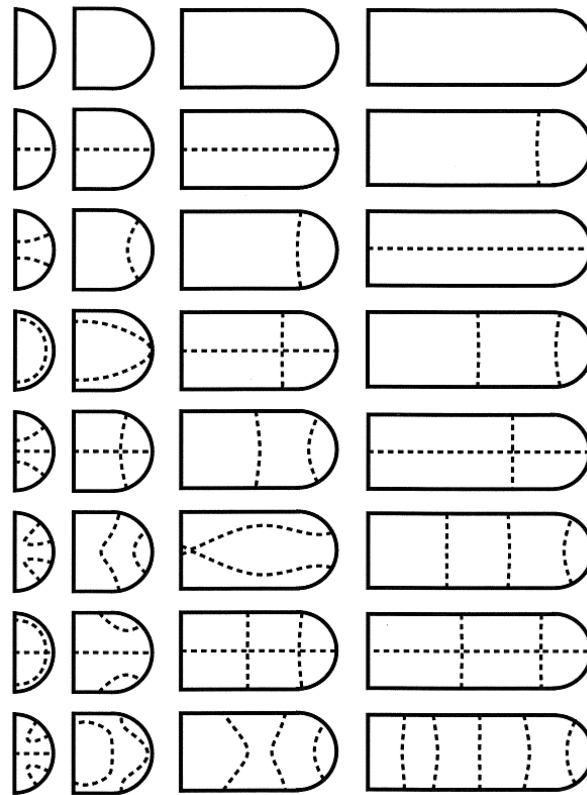


Figure 3. First eight vibration modes of the long cantilever plate. The left edge is clamped. Dashed lines denote nodal curves. From left:  $a = 0, 1, 3, 5$ .

Figure 3 shows the vibrational modes for the long cantilever plate. The plate is clamped at the left straight side while the remaining boundaries are free. The fundamental mode has no interior

nodal curves, or the plate has a flapping motion. The second mode is anti-symmetric (twisting) for small  $a$  but switches to the symmetric (up-down) mode when  $a = 5$ . More switches occur for higher modes. For larger aspect ratios, we expect the vibrations are dominated by the symmetric modes. Figure 4 shows the three-dimensional mode shapes for a long cantilever plate. Note the twisting vibrations of the third and fifth modes.

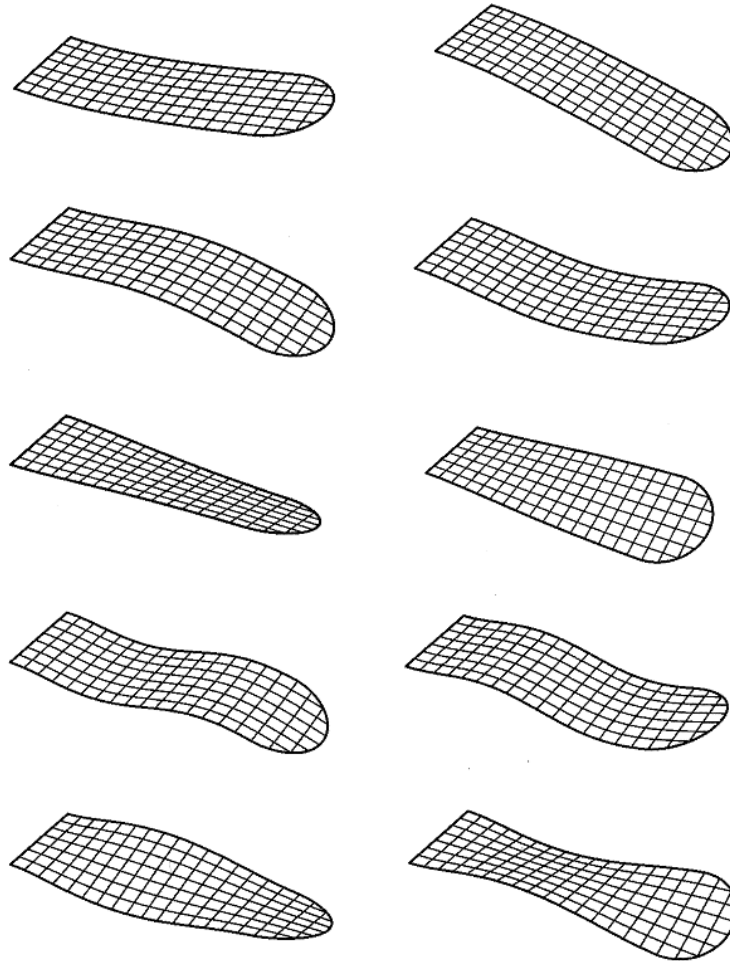


Figure 4. Three-dimensional vibration modes of the long cantilever plate ( $a=5$ ). The left edge is clamped. Note the first, second, and fourth modes are flapping modes, while the third and fifth modes are twisting modes.

When  $a = 0$ , it is the semicircular plate clamped at the straight edge. Figure 5 shows some three-dimensional displacements of the semi-circular cantilever plate. Note the second and fifth modes are twisting vibrations.

For the wide cantilever plate of Figure 1c, the plate is clamped on the major axis ( $x$ -axis) while the rest of the boundaries are free. The aspect ratio is  $2(a+1)$ . Table 6 shows the first eight frequencies.

Figure 6 shows the mode shapes. Note that for larger aspect ratios the nodal curves are mostly transverse to the (clamped) major axis. Figure 7 shows typical three-dimensional vibration modes.

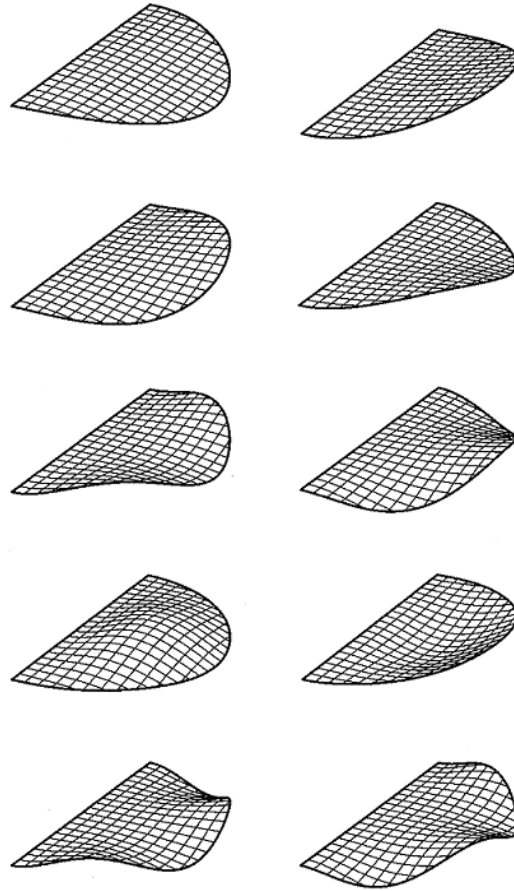


Figure 5. First five modes of the vibration of the semi-circular cantilever plate. The first, third and fourth modes are symmetric modes (with respect to the bisecting axis), and the second and fifth modes are anti-symmetric.

Table 6 First eight frequencies of the wide cantilever plate. Aspect ratio is  $2(a+1)$ . Subscripts denote mode shape.

$a$	0	0.5	1	2	3
$k$	4.5384S	3.996S	3.805S	3.661S	3.605S
	9.3561A	6.253A	5.048A	4.200A	3.909A
	17.229S	10.32S	7.441S	5.255S	4.487S
	27.016S	15.96A	10.84A	6.823A	5.360A
	27.581A	22.39S	15.15S	8.883S	6.529S
	40.264S	22.33S	20.17A	11.38A	7.919A
	41.950A	32.10A	23.12S	14.77S	10.04S
	55.191A	37.03S	25.88A	17.90A	11.49A



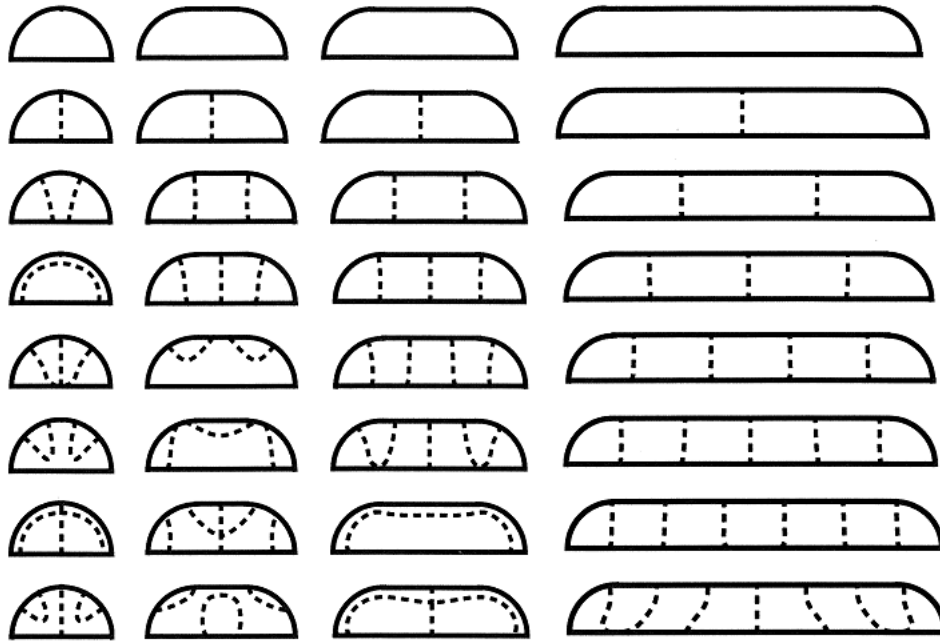


Figure 6. First eight vibration modes of the wide cantilever plate. The bottom edge is clamped. Dashed lines denote nodal curves. From left:  $a = 0, 1, 3, 5$ .

Let us compare the vibration of rectangular plates and that of rectangular plates with rounded ends. Let the area be the same, such that the effective surface, be it solar panel or lifting wing, be of same area. For the same width, the rectangle length is  $c$ , related to the rounded rectangle by  $c = a + \pi/4$ . Table 7 shows a comparison of the first four frequencies for the completely free plate. Table 8 shows the comparison for the cantilever plates.

Table 7 Comparison of the frequencies of the completely free rounded rectangular plate and the rectangular plate of same area (with asterisk).

$a = 0.5$	$a = 1$	$a = 2$	$a = 3$	$a = 4$	$a = 5$
2.789	1.564	0.671	0.368	0.231	0.159
3.220*	1.683*	0.691*	0.374*	0.234*	0.160*
3.082	2.108	1.274	0.911	0.636	0.437
2.614*	1.867*	1.181*	0.862*	0.647*	0.442*
6.605	4.094	1.823	1.009	0.709	0.580
5.584*	4.561*	1.920*	1.037*	0.679*	0.560*
6.871	4.701	2.772	1.901	1.244	0.856
7.464*	4.175*	2.509*	1.793*	1.275*	0.870*

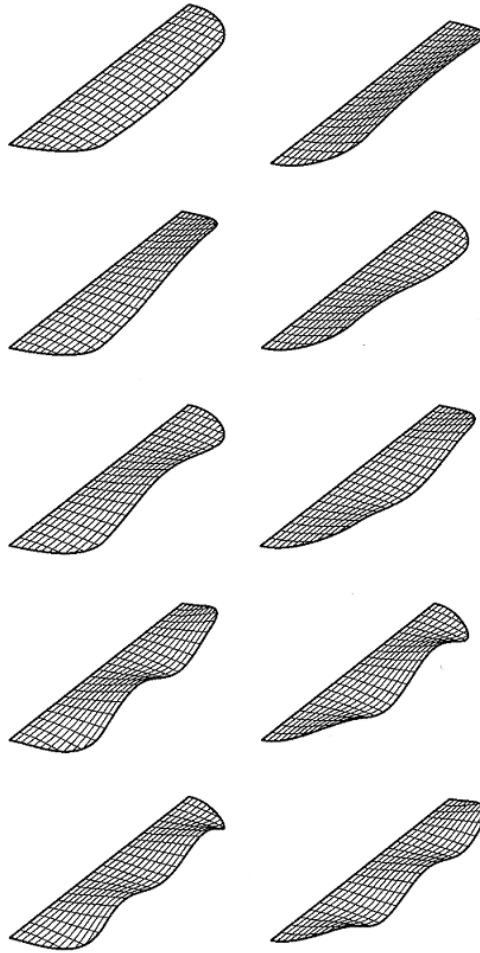


Figure 7. First five modes of the vibration of the wide cantilever plate ( $a = 2$ ).  
The first, third and fifth modes are symmetric, and the second and fourth modes are anti-symmetric.

Table 8. Comparison of the frequencies of the cantilever rounded rectangular plate and the cantilever rectangular plate of same area (with asterisk).

$a = 0.5$	$a = 1$	$a = 2$	$a = 3$	$a = 4$	$a = 5$
1.939	1.044	0.438	0.238	0.149	0.102
2.111*	1.092*	0.447*	0.241*	0.150*	0.103*
4.579	2.845	1.550	1.051	0.784	0.631
3.778*	2.45*	1.417*	0.967*	0.755*	0.639*
9.208	5.675	2.597	1.448	0.916	0.635
8.352*	6.482*	2.759*	1.498*	0.936*	0.612*
13.35	9.211	5.239	3.449	2.534	1.752
13.264*	7.352*	4.831*	3.231*	2.628*	1.795*

Note that if the edges are rounded, the fundamental (symmetric) frequency is slightly decreased,

while the second frequency (usually antisymmetric) may be slightly increased or decreased. The differences in frequencies become even smaller when the aspect ratio becomes larger. Thus rounding the ends has definite advantages in increased structural strength while the frequency change little.

#### 4. Discussions and conclusion

The boundary conditions of a free edge on a plate are zero moment and zero shear. From e.g. [12, 13] the expressions are

$$M_n = -D \left\{ (1-\nu) [w_{xx} n_{(x)}^2 + 2w_{xy} n_{(x)} n_{(y)} + w_{yy} n_{(y)}^2] + \nu (w_{xx} + w_{yy}) \right\} = 0 \quad (13)$$

$$V_n = D \left\{ \begin{aligned} (1-\nu) \frac{\partial}{\partial s} [ (w_{xx} - w_{yy}) n_{(x)} n_{(y)} - w_{xy} (n_{(x)}^2 - n_{(y)}^2) ] \\ - (w_{xxx} + w_{xyy}) n_{(x)} - (w_{yyy} + w_{yxx}) n_{(y)} \end{aligned} \right\} = 0 \quad (14)$$

here  $n_{(x)}$ ,  $n_{(y)}$  are components of the unit normal, and  $s$  is the unit tangent direction. These boundary conditions present serious challenges if they are to be enforced, for methods such as finite differences, finite elements [16], infinite series expansions [17] or discrete singular convolution [18]. This is probably the reason these methods are rarely used for plates with curved free edges, even for the semi-circular cantilever plate. However, the present modified Ritz method automatically satisfies the free vibration boundary conditions [11], thus is well suited for free (curved) edge problems. Note that unlike the rectangular or elliptic geometry, the Ritz method cannot be used for the stadium geometry if the edges are clamped or simply-supported, due to the circular arc boundary.

Using proper mode classifications, the first eight frequencies and mode shapes are computed. For the completely free stadium-shaped plate, the fundamental mode always has two nodal curves transverse to the major axis. The second mode has perpendicular nodal lines along both axes for  $a < 3.5$  but switches to three transverse nodal curves for  $a > 3.5$ . There are numerous switches for the higher modes. For the long cantilever plate the fundamental mode has no internal nodal curves, i.e. a flapping motion. The second mode is a twisting oscillation for  $a < 4.95$ , but switches to flapping (with one transverse nodal curve) for  $a > 4.95$ . For the wide cantilever plate the fundamental mode is always flapping, and the second mode is always twisting.

The contributions of the present work include firstly the accurate archival frequencies of the important stadium-shaped plate, and secondly the detailed descriptions of the vibration modes. These frequencies and mode shapes, obtained by our efficient modified Ritz method, are essential in the design of completely free or cantilevered plates.

#### References

- [1] C.Y. Wang and C.M. Wang, Structural Vibration: Exact Solutions for Strings, Membranes, Beams, and Plates, CRC Press, Boca Raton, FL, 2014.
- [2] A.W. Leissa, Vibration of Plates, NASA Washington D.C. Report SP-160, 1969.
- [3] R.D. Blevins, Formulas for Natural Frequency and Mode Shape, Kreiger, FL, 1993.
- [4] B. Wie and C.M. Roithmayr, Attitude and orbit control of a very large geostationary solar power satellite, J. Guid. Control Dyn. 28, pp. 439-451, 2005.

- [5] C.M. Wang and Z.Y. Tay, Very large floating structures: Applications, research and development, Proc. Eng. 14, pp. 62-72, 2011.
- [6] A.W. Leissa, The historical bases of Rayleigh and Ritz methods, J Sound Vibr. 287, pp. 961-978, 2005.
- [7] T. Irie, G. Yamada and M. Sonoda, Natural frequencies of square membrane and square plate with rounded corners, J. Sound Vibr. 86, pp. 442-448, 1983.
- [8] C.Y. Wang, Vibrations of completely free rounded rectangular plates, J. Vibr. Acoust. 137, p. #024502, 2015.
- [9] C.W. Kim and K.M. Liew, Effects of boundary constraints and thickness variation on the vibratory response of rectangular plates, Thin-Walled Struct. 17, pp. 133-159, 1992.
- [10] B. Singh and V. Saxena, Transverse vibration of a quarter of an elliptic plate with variable thickness, Int. J. Mech. Sci. 37, pp. 1103-1132, 1995.
- [11] K.M. Liew and C.M. Wang, Pb-2 Rayleigh- Ritz method for general plate analysis, Eng. Struct. 15, pp. 55-60, 1993.
- [12] S. Timoshenko and S. Woinowsky-Krieger, Theory of Plates and Shells, McGraw-Hill, New York, 1959.
- [13] K. Washizu, Variational Methods in Elasticity and Plasticity, Pergamon, Oxford, UK, 1982.
- [14] O.G. McGee, A.W. Leissa, C.S. Huang and J.W. Kim, Vibrations of circular plates with clamped V-notches or rigidly constrained radial cracks, J. Sound Vibr. 181, pp. 185-201, 1995.
- [15] R.A. Westmann, A note on the free vibrations of triangular and sector plates, J. Aerosp. Sci. 29, pp. 1139-1140, 1962.
- [16] A. Houmat and M.M. Rashid, Coupling of h and p finite elements: Application to free vibration analysis of plates with curvilinear plan forms, Appl. Math. Modeling 36, pp. 505-520, 2012.
- [17] X. Shi, D. Shi, W.L. Li and Q. Wang, A unified method for free vibration analysis of circular, annular and sector plates with arbitrary boundary conditions, J. Vibr. Control 22, pp. 442-456, 2016.
- [18] O. Civalek, Use of eight-node curvilinear domains in discrete singular convolution method for free vibration analysis of annular sector plates with simply-supported radial edges, J. Vibr. Control 16, pp. 303-320, 2010.